

1 Probing the chemical transformation of seawater- 2 soluble crude oil components during microbial 3 oxidation

4 Yina Liu ^{1,†,×,#,*}, Helen K. White [‡], Rachel L. Simister [‡], David Waite [§], Shelby L. Lyons [‡],
5 Elizabeth B. Kujawinski ¹

6 ¹Department of Marine Chemistry & Geochemistry, Woods Hole Oceanographic Institution,
7 Woods Hole, Massachusetts, United States

8 [‡]Geochemical and Environmental Research Group, Texas A&M University, College Station,
9 Texas, United States

10 [×]Department of Oceanography, Texas A&M University, College Station, Texas, United States

11 [‡]Department of Chemistry, Haverford College, Haverford, Pennsylvania, United States

12 [§]School of Biological Sciences, University of Auckland, Auckland, New Zealand

13 * Corresponding author: Yina Liu, yina.l.liu@gmail.com

14 # Present address: Geochemical and Environmental Research Group, Texas A&M University,
15 College Station, Texas, United States

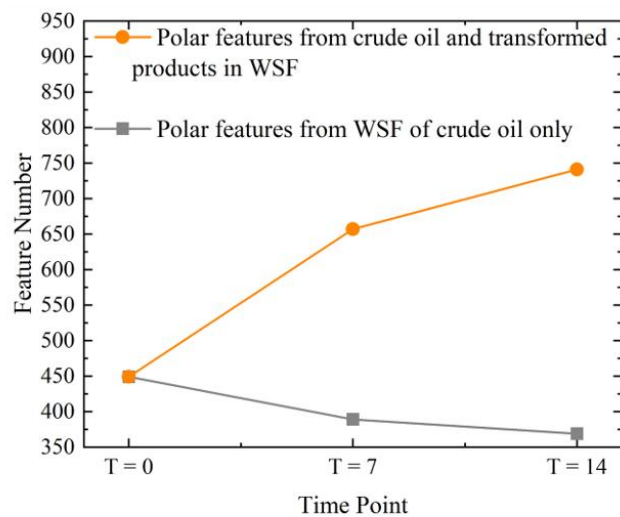
16

17

TOC Art



Water-Soluble Fraction (WSF)



Incubation experiment

18

19

20

21 ABSTRACT

22 Studies assessing the environmental impacts of oil spills focus primarily on the non-water-soluble
23 components, leaving the fate of the water-soluble fraction (WSF) largely unexplored. We
24 employed untargeted chemical analysis along with biological information to probe the
25 transformation of crude oil WSF in seawater, in the absence of light, in a laboratory experiment.
26 Over a 14-day incubation, microbes transformed WSF into various metabolic intermediates,
27 without significantly altering the dissolved organic carbon concentrations. Microbial
28 transformation processes increased the chemical diversity and overall oxygen content of WSF
29 compounds, concomitant with an increase in dioxygenase gene abundances. While the majority of
30 metabolites formed from the transformation of WSF could not be structurally identified with
31 existing databases, elemental formulas suggest that many of these compounds could be oxidation
32 products of water-soluble non-polar compounds such as PAHs. In particular, metabolites with
33 three oxygen atoms may represent a key transition point for WSF degradation. One such
34 compound, salicylic acid, likely provides a route for complete WSF remineralization, as it is labile
35 to non-oil degrading marine bacteria. The environmental persistence and toxicity of WSF
36 metabolic products are still unknown, but results from this study provide a framework for further
37 exploration of the fate of WSF in marine ecosystems.

38
39

40 INTRODUCTION

41 Millions of barrels of crude oil are released to the ocean each year from unintentional spillages
42 and natural seepage.¹ A small, but significant, fraction of the oil dissolves in the water and behaves
43 differently than the bulk oil. The composition of dissolved oil is distinct from the total oil and is
44 enriched in small (<1000 Da), polar molecules.² Despite decades of study on the fate of oil in the
45 environment, the water-soluble fraction (WSF) is vastly understudied because its components are
46 not resolved in traditional gas-chromatography (GC)-based analytical methods. Consequently, we
47 know much less about the factors affecting the fate and transport of crude oil WSF in marine
48 ecosystems, despite evidence suggesting that this fraction is enriched during weathering and is
49 more toxic to aquatic organisms than the parent oil.³⁻⁶

50 WSF can be preferentially enriched in the aqueous phase at any oil-water interface, such as in
51 surface waters in contact with oil slicks, seawater around oil seeps or deep-sea oil spills, as well
52 as in water-inundated oil-contaminated soil. The best-studied case for such oil-water partitioning
53 phenomena was at the *Deepwater Horizon* (DWH) drill site in 2010, where 3.19 million barrels of
54 oil spilled into the Gulf of Mexico over a period of 87 days.⁷ Unlike many major oil spills, crude
55 oil from the Macondo well was injected into the water column from the deep-sea. A widespread
56 neutrally buoyant subsurface plume, as thick as 200 m, was observed at 1100 m depth and persisted
57 for months after the blowout.⁸ Assessments during the early response estimated that water-soluble
58 crude oil components were preferentially enriched in this subsurface plume,⁹ with water-soluble
59 hydrocarbons such as low molecular weight n-alkanes and monoaromatic hydrocarbons
60 comprising ~69% by mass.^{8, 10, 11} The preferential enrichment of crude oil WSF in the deep ocean
61 underscores dissolution as an important process driving the distribution of spilled oil.⁹

62 The transport, ecotoxicological impacts, and biotic and abiotic degradation of oil have been the
63 central focus of many oil-spill studies.^{9, 12-18} Microbial degradation represents one of the key
64 degradation pathways for crude oils, and thus has been investigated for decades.¹⁹⁻²⁵ Microbial
65 composition and oil degradation pathways deduced from genome sequences and transcripts have
66 previously been investigated in diverse impacted marine ecosystems.^{11, 16, 17, 24, 26, 27} These studies
67 frequently focus on biologically-mediated chemical transformations and degradation of major
68 compound classes in crude oils, such as n-alkanes, monoaromatic compounds (benzene, toluene,
69 ethylene, and xylene, or BTEX), and polycyclic aromatic hydrocarbons (PAHs).^{12, 28-30} Absent
70 from these studies, however, is information on the microbial response specific to the subset of
71 crude oil that is truly dissolved in water and more polar than hydrocarbons, i.e. compounds that
72 contain heteroatoms (N, S, and O).

73 Polar compounds account for <15% by mass in bulk crude oil,³¹ but may account for a
74 substantial fraction (70-82%) of the water-soluble fraction (WSF),^{3, 32} depending on the oil type
75 and extent of weathering.

76 Recent studies examining the dissolution of crude and weathered oils in seawater have improved
77 understanding of the chemical composition of WSF.^{2, 33, 34} NSO-containing compounds are more
78 polar than hydrocarbons, preferentially partition into seawater^{2, 33} and appear to be resistant to
79 biodegradation and toxic to organisms.^{3, 9} For example, uncharacterized compounds from WSF
80 fractions generated from microbial degradation of crude oil were found to be toxic to marine
81 organisms such as Crustacea,⁵ highlighting the critical gap in understanding WSF chemical
82 composition and its biogeochemical transformations in the context of ecotoxicity affecting the
83 marine food web. The microbial response to WSF, however, is relatively unexplored, particularly
84 in comparison to responses to BTEX,^{35, 36} PAHs,^{37, 38} and alkanes.^{24, 35} More recently, next-

85 generation sequencing was employed to examine the sequential dominance of hydrocarbon
86 degraders in conjunction with traditional and emerging assessments of oil degradation, but these
87 tools were unable to link directly to WSF chemistry.^{11, 14, 17, 39}

88 Complex mixture analysis enabled by advanced mass spectrometry methods can provide
89 valuable information on the composition and fate of spilled oils, particularly the polar fraction
90 contained in WSF. Ultrahigh-resolution mass spectrometry such as Fourier transform ion cyclotron
91 resonance mass spectrometry (FT-ICR MS) can be widely used in response to the spills and crude
92 oil characterizations, providing insight into crude oil-derived compounds that could not be
93 resolved with GC-based methods.^{2, 28, 29, 31, 33, 34, 40-44} When applied to biological systems, these
94 analytical techniques identify and quantify molecules produced by organisms, thus providing
95 metabolite profiles of microbial cultures or communities under various conditions.^{26, 28}

96 In this study, we employ untargeted metabolite profiling, guided by biological information (16S
97 rRNA gene and metagenomics), to examine the evolving chemical signature of WSF and the
98 dynamics of polar crude oil compounds within dark aerobic incubations with natural seawater
99 bacterial consortia. This approach combined with existing knowledge of hydrocarbon degradation
100 pathways enabled us to explore the microbial mechanisms responsible for WSF degradation in
101 aerobic seawater.⁴⁵

102

103 EXPERIMENTAL SECTION

104 **Incubation Experiment.** We created WSF by slow dissolution of Macondo oil surrogate
105 (source crude oil – MC252; Item IDs A0067V and A0067X) in 0.2 µm-filtered Vineyard Sound
106 seawater (VSW), following the low energy mixing methods described in Liu and Kujawinski²
107 (Supporting Information and Figure S1a). Briefly, we loaded the Macondo oil surrogate on the

108 surface of VSW at a 5:95 (v/v) ratio and allowed the oil dissolution to occur over 7 days in the
109 dark at room temperature. Low energy (i.e., a slow-moving stir bar) was applied to ensure
110 exchange across the water column, but no oil droplets were entrained into the water. After 7 days,
111 we filtered the resulting water-accommodated fraction (WAF) through a 0.7 μm glass fiber filter
112 (GF/F) to collect the truly water-soluble oil component (i.e. WSF). Volatile hydrocarbons such as
113 benzene, toluene, ethylbenzene, and xylene (BTEX) are not retained in this protocol, as they
114 evaporate over the 7-day mixing period or are lost during the filtration process. Thus, this method
115 captures primarily low molecular weight PAHs and polar, water-soluble compounds. The
116 dissolved organic carbon (DOC) concentration of WSF was comparable to that observed in the
117 field during DWH spill (Figures S3).⁴⁶

118 We established three parallel treatments, each in triplicate, to explore microbial community
119 changes in response to the addition of crude oil-derived components in the WSF (Figures S1b):
120 (1) the VSW control, which contained background seawater dissolved organic matter (DOM) and
121 natural bacterial consortia; (2) the succinic acid treatment, which contained seawater DOM,
122 succinic acid, and natural bacterial consortia; and (3) the WSF treatment, which contained seawater
123 DOM, crude oil WSF, and natural bacterial consortia. Succinic acid was used as a labile carbon
124 substrate control to distinguish opportunistic microbes responding to carbon addition,⁴⁷ from oil-
125 degrading microbes responding uniquely to WSF components. In treatments (2) and (3), we added
126 the organic substrates at similar DOC concentrations (succinic acid = $347 \pm 7 \mu\text{M-C}$; WSF $311 \pm$
127 $7 \mu\text{M-C}$).

128 We added 0.2 μm -filtered ammonium chloride (NH_4Cl ; 4 nM) and sodium phosphate (NaH_2PO_4 ;
129 0.3 nM) to all incubation chambers to mitigate nutrient limitation for cell growth. We inoculated
130 each treatment with natural bacterial consortia at a volume ratio of 10%, at the beginning of the

131 experiment (Supporting Information). One liter of headspace remained in each incubation
132 chamber, and we maintained aerobic conditions by swirling the incubation chambers gently three
133 times daily. We kept all incubations in the dark at room temperature (~24°C) throughout the 14-
134 day experiment. The experiment was conducted in the dark to minimize photo-oxidation;^{12, 48}
135 consequently, the observed chemical signatures over the experiment should be due primarily to
136 heterotrophic transformations. The lab conditions chosen for this experiment prioritized our aim
137 to examine microbial oxidation at a rate that would yield measurable metabolites in 14 days, before
138 significant bottle effects occurred. Therefore, the experimental temperature was higher than deep-
139 sea conditions, although still relevant to surface ocean conditions. Additional details on the
140 experiment setup are provided in the Supporting Information.

141 **Sample Collection, Preparation, and Analyses.** We collected samples on three days (0, 7, 14).
142 On the sampling day, we swirled each bottle gently to ensure homogeneity and then filtered each
143 sample through a 0.2 µm Omnipore (Millipore Sigma) membrane filter under low vacuum. We
144 used filtrates for external metabolite profiling, PAH analysis, and dissolved organic carbon (DOC)
145 analysis. We used microbial biomass retained on the filter for 16S rRNA gene and metagenomics
146 analyses. We enumerated bacteria in 10 mL of unfiltered water that was fixed with borate-buffered
147 formalin (2% final concentration) and frozen at -20°C. Our WSF protocol includes GF/F filtration
148 to remove oil droplets² and thus we do not expect significant amounts of hydrophobic or sparingly
149 hydrophilic compounds to be retained on the 0.2-µm membrane filters used for biomass collection.
150 We stored the filters at -80°C until extraction.

151 We acidified the filtrates (2L) to pH ~3 immediately after filtration, extracted the samples with
152 PPL solid-phase extraction (SPE) cartridges (Bond Elut, Agilent), and then eluted with 100%
153 methanol as described in Dittmar et al.⁴⁹ and modified by Longnecker.⁵⁰ The eluents were stored

154 at -20°C until mass spectrometry analysis. Immediately before analysis, we dried down the eluents
155 to near dryness and reconstituted them in 250 µL of 95:5 water:acetonitrile. We added deuterated
156 biotin (5 µL; final concentration 0.05 µg/mL) to each sample as an internal standard. PPL resins
157 preferentially capture the aromatic compounds in WSF, but do not retain very small, highly polar
158 molecules such as succinic acid.⁵¹ Therefore, to ensure similar extracted carbon concentrations
159 across all treatments and within the pooled samples, we diluted the WSF treatment eluents 50×
160 due to high concentrations of extracted carbon relative to the non-WSF treatments. We combined
161 50 µL of each sample to create a pooled sample as a reference for data quality control and
162 processing.

163 We divided all samples into two equal volumes, one for targeted analysis and one for untargeted
164 analysis, following methods described by Kido Soule et al.⁵² The untargeted approach, using liquid
165 chromatography coupled to FT-ICR MS (LC-FT-ICR MS) equipped with an electrospray
166 ionization (ESI) source, allows examination of metabolite profiles without prior knowledge of
167 sample composition, and thus enables simultaneous identification of known compounds and
168 discovery of previously unknown metabolites. Metabolite profiles from different incubation
169 conditions at the three time points provided valuable information on how the microbes transformed
170 WSF components compared to other organic substrates over the 14-day experiment. Here, we
171 define a metabolite profile as all the features in a given sample, where a feature is defined as a
172 unique combination of mass to charge ratio (m/z) and retention time (RT). Each feature
173 corresponds to a specific metabolite or to a group of co-eluting isomers.

174 We subjected the top four features in each mass scan to tandem mass spectrometry (MS/MS or
175 MS²) for compound identification. We applied rigorous data quality control procedures to ensure
176 data robustness, e.g. removing features whose variability is driven by instrumental parameters

177 and/or are consistently present in all samples at similar intensities (see Supporting Information).
178 After these measures, approximately 40-48% of features in the dataset had associated MS2 spectra.
179 We used a step-wise approach to classify metabolites of interests based on the Metabolomics
180 Standards Initiative's (MSI) established four-level standard.⁵³ Specifically, a level-4 classification
181 includes unknown features that passed QA/QC but do not match any literature and database values;
182 a level-3 putative characterization requires a match between observed exact mass values and
183 elemental formulas; and a level-2 putative annotation requires a multi-component match between
184 exact mass and other physicochemical properties (e.g. RT and/or fragmentation pattern) with
185 literature or external libraries. The highest confidence level-1 identification requires at least two
186 of four independent confirmations of RT, exact mass, MS2 spectrum, or isotope patterns from a
187 chemical standard under identical analytical conditions.⁵³ We used the MetFrag *in silico* tool⁵⁴ to
188 search the fragmentation patterns and exact mass values to generate level-2 putative annotations.
189 We compared the search results with metabolites listed in Kyoto Encyclopedia of Genes and
190 Genomes (KEGG) for key hydrocarbon degradation pathways. For pathways with multiple level-
191 2 putative annotations, we searched our feature list for additional level-3 putative characterizations
192 within these pathways. We assigned elemental formulas for the level-3 features using an automated
193 compound identification algorithm (CIA) as described in Kujawinski and Behn⁵⁵ with parameters
194 from Liu and Kujawinski.² We did not consider pathways with only level-3 putative
195 characterizations, due to the inability to distinguish among structural isomers with the same mass.
196 Finally, we confirmed level-1 identities of key metabolites with commercial standards, including
197 six intermediates related to degradation of naphthalene and methylnaphthalenes, namely 3- and 4-
198 hydroxybenzaldehyde, salicylic acid, 3- and 4-methylsalicylic acid, and gentistic acid. These
199 metabolites were then quantified by LC triple-quadrupole-MS (see Supporting Information).

200 It should be noted that many observed features could not be identified with literature or database
201 searches (i.e. level-4). Additionally, many level-2 and level-3 features do not have commercial
202 standards available. Due to the lack of appropriate standards for most of the detected features,
203 feature intensities obtained with the untargeted method could not be converted to absolute
204 concentrations. Instead, we used relative abundances to compare concentration changes among
205 samples. We calculated relative abundance as: $\Sigma(\text{Intensity of feature groups}) / \Sigma(\text{Intensity of all}$
206 $\text{detected features}) \times 100$, where feature groups can be defined as specific compound classes or
207 those that contained elements of interest such as oxygen.

208 Compounds ionizable by ESI contain at least one polar function group; thus, features detected
209 by LC-FT-ICR MS are, by analytical definition, more polar than hydrocarbons containing no polar
210 functional groups. Therefore, we equate polar compounds with those observed within the LC-FT-
211 ICR MS analytical window in the subsequent discussions.

212 **Sample Collection for PAH Analysis.** We extracted 100 mL of WSF samples with
213 dichloromethane (DCM) for PAH analysis. We dried the extracts with anhydrous Na_2SO_4 and
214 removed excess DCM by rotary evaporation. We reconstituted the concentrated samples with
215 toluene for global chemical characterization through direct infusion FT-ICR MS (data not shown).
216 We took aliquots of $\sim 250 \mu\text{L}$ from the remaining samples in toluene and performed solvent
217 exchange by drying down the toluene under a gentle stream of high purity nitrogen. The dried
218 samples were shipped to Haverford College for PAH analysis. The samples were reconstituted
219 with DCM before analysis by GC-MS. We expect that our PAH concentrations are underestimates
220 due to the sample drying steps. For example, naphthalene was not detected, which is inconsistent
221 with this oil's known composition.⁵⁶ From previous work, we expect the less volatile PAHs should
222 account for $\sim 10\%$ of the WSF.³ Individual PAH analyzed in this study included: naphthalene, C1-

223 C4 alkylated naphthalenes, biphenyl, fluorene, C1-C3 alkylated fluorenes, dibenzothiophene, C1-
224 C3 alkylated dibenzothiophenes, anthracene, C1-alkylated anthracene, phenanthrene, C1-C3
225 alkylated phenanthrenes, chrysene, C1-C3alkylated chrysenes, and triphenylene and
226 benzo(a)anthracene. Detailed method for PAH analysis is described in the Supporting Information.

227 **16S rRNA Gene and Metagenomics Analysis.** We extracted microbial DNA from all filters
228 using the MO BIO PowerWater (PW) kit (MOBIO Laboratories, Inc., Carlsbad, CA), according
229 to the manufacturer's instructions. Purified genomic DNA was submitted to the University of
230 Wisconsin-Madison Biotechnology Center. Further details of sample preparations for 16S rRNA
231 gene and metagenomics sequencing, library construction and bioinformatics analysis are provided
232 in Supporting Information.

233

234 RESULTS AND DISCUSSION

235 **Presence of WSF Selected for Distinct Microbial Communities.** Both chemical and microbial
236 community compositions within the same treatment type changed between the initial time point
237 and 7 and/or 14 days (Figures S2a and b), indicating selection of microbial community based on
238 the organic substrates and microbial alteration of the organic compounds in the starting incubation
239 media. Among the three treatments, the chemical and microbial community compositions were
240 different between non-WSF (i.e. VSW and succinic acid) and WSF incubations (Figures S2a and
241 b). The use of succinic acid as a control carbon source allowed us to determine that this observed
242 shift in microbial community is due specifically to the addition of WSF and not due to
243 opportunistic microbes. Indeed, we observed known hydrocarbon degraders uniquely in the WSF
244 treatment, including *Cycloclasticus*, *Oceaniserpentilla*, and *Rhodospirillales*, consistent with field
245 observations of microbial diversity during the DWH spill (Table S5 and S6).^{11, 24, 57}

246 **WSF is Transformed in Incubation Experiments.** We used changes in DOC concentrations
247 across time points to evaluate complete remineralization of organic carbon to CO₂ in each
248 treatment. DOC values were not statistically significantly different across the 14-day incubation
249 in the WSF treatments, based on a one-way ANOVA test at 95% confidence level (Figure S3). In
250 contrast, DOC concentrations decreased more than 100 μM-C by T = 14 in the succinic acid
251 treatment, suggesting catabolism of succinate for energy (Figure S3). DOC concentrations in the
252 VSW treatment were also not statistically significantly different across the three time points, which
253 was likely due to the overall lower biomass and microbial activity as a result of lower DOC
254 concentrations (Figures S4).

255 We used LC-FT-ICR MS to examine detailed chemical changes as the microbes altered WSF.
256 We define polar WSF-derived chemical features (P-WSF_{Total}), resolved by LC-FT-ICR MS, to be
257 those found in WSF treatment but not in any non-WSF treatments. We culled the list of features
258 to those that were found in all replicates at a time point. We then divided P-WSF_{Total} into P-WSF₀,
259 or the polar WSF compounds found at T = 0, and P-WSF_M, or the polar metabolites produced
260 during microbial degradation of WSF compounds (Figure S5).

261 To understand the chemical dynamics within WSF over the course of our experiment, we further
262 subdivided P-WSF₀ into four groups: P-WSF_{0-C}, or features that were likely consumed completely
263 (present only at T = 0); P-WSF_{0-U}, or features that were **unaltered** (similar relative abundance
264 values over 14 days); P-WSF_{0-I}, or features whose relative abundances **increased** over 14 days; and
265 P-WSF_{0-D}, or features whose relative abundances **decreased** over 14 days. The last three groups
266 (P-WSF_{0-U}, P-WSF_{0-I}, and P-WSF_{0-D}) include features present in WSF treatment samples at all
267 time points. We based our feature classifications on pair-wise one-tailed Student's t-test of feature
268 intensities. A visual overview of our classification scheme is shown in Figure S5.

269 Overall, the features in P-WSF_{Total} increased from 449 at T = 0 to 741 at T = 14 (Figure 1; Table
270 S1), indicating formation of new compounds as a result of microbial transformation of WSF crude
271 oil. Only 80 of 449 (<18 %) P-WSF₀ features were missing by the end of the experiment, due
272 either to complete degradation or to reduction below the detection limit (Figure 1; Table S1). In
273 contrast, P-WSF_M accounted for 41% and 50% of the total features observed in T = 7 and 14,
274 respectively (Tables S1 and S2). The similarity in DOC concentrations in WSF treatment samples
275 across time points, together with the increase in the number of P-WSF_{Total} and the small fraction
276 of P-WSF_{0-C}, implies that the majority of compounds initially found in WSF were transformed
277 into metabolic intermediates by microbial degradation rather than completely remineralized to
278 CO₂, within the time frame of the experiment.

279 Changes in the relative abundances of features in P-WSF_{0-I} and P-WSF_{0-D} were significant
280 between T = 0 and T = 7 but not significant between T = 7 and T = 14, based on paired one-tailed
281 Student's t-tests (Figure 2 and Table S3). In contrast, increases in relative abundances for P-WSF_M
282 features were significant between T= 0 and T = 7, and between T = 7 and T = 14 (Figure 2 and
283 Table S3). These findings suggest that processes that lead to a decrease or increase in abundances
284 of P-WSF₀ features proceed at slower rates, or not at all, after T = 7; while production of P-WSF_M
285 continues after T = 7 and potentially beyond T = 14. The source of P-WSF_M may be P-WSF₀ and/or
286 low-molecular weight, water-soluble non-polar compounds, such as PAHs. We can discount the
287 first possibility because the change in relative abundance in P-WSF_{0-D} is minimal between T = 7
288 and T = 14. In contrast, the second possibility could only be explained by microbial oxidation of
289 compounds that were originally outside the LC-FT-ICR MS analytical window, such as the non-
290 polar compounds in WSF.

291 **Degradation of PAHs is a Likely Source of Polar Metabolites in WSF.** One of the possible
292 sources of P-WSF_M is the oxidation of non-polar compounds. To investigate whether non-polar
293 compounds in WSF are the sources of polar compounds, we focused our data interpretation on the
294 degradation of water-soluble PAHs, i.e. typically those with less than 3-rings, which should
295 account for ~10% of the WSF.³ If all or a major fraction of PAHs were completely remineralized
296 into CO₂, such a process should result in statistically significant changes in DOC concentrations.
297 However, DOC concentrations did not change significantly while total PAH concentration
298 decreased and the number of P-WSF_{Total} increased (Figures 1 and S6). These observations support
299 the notion that the source of the increasing P-WSF_M was likely the non-polar compounds that were
300 not detected by LC-FT-ICR MS at T = 0.

301 We identified a total of 56 metabolites that occur within known aerobic aromatic compound
302 degradation pathways, such as xylene, toluene, naphthalenes, and PAHs with three or fewer rings
303 (Table S4). Twenty-four of the 56 compounds from P-WSF_{Total} were assigned a level-2 putative
304 annotation based on exact mass and fragmentation pattern matches (Table S4). Of the 24 Level-2
305 metabolites, 7 were associated with the degradation of naphthalene and methyl-naphthalenes
306 (Table S4), even though naphthalene was not detected in PAH analysis. Multiple naphthalene
307 degradation products were observed across all time points with either negligible abundances at T
308 = 0 and elevated abundances at T=7 and/or T=14 or with the highest abundances at T = 7 (e.g.
309 Figures S7 and S8). We observed multiple metabolites from the degradation of aromatic
310 compounds with 1-3 rings, but no metabolites associated with the degradation of high molecular
311 weight PAHs. This is consistent with the absence of high molecular weight PAHs in WSF based
312 on their low aqueous solubilities.²

313 **O3 and O4 Metabolites are Important Intermediates in WSF Transformations.** The number
314 of putatively annotated compounds related to WSF degradation accounted for only a small
315 percentage (<12%) of P-WSF_{Total} in each sample. To better understand the characteristics of the
316 broad range of compounds observed in WSF, existing chemical reaction information available in
317 the KEGG database and metagenomics data from this study was used to guide the interpretation
318 of the remaining P-WSF_{Total} features.

319 We focused on P-WSF_{Total} features with assigned formulas (Levels 1, 2, and 3) that contained
320 oxygen atoms, since oxidation is a well-known mechanism for oil degradation. Aerobic
321 biodegradation of PAHs is catalyzed by either monooxygenases or dioxygenases, enzymes that
322 add one or two oxygen atoms, respectively, in the initial steps.^{38, 58-61} In bacteria, dioxygenases are
323 the primary enzymes that initiate the PAH degradation.^{38, 59, 62} For PAHs with three or fewer rings,
324 dioxygenase-catalyzed oxygen addition occurs up to four oxygen atoms (O4), at which point one
325 ring opens. The open-ring O4 intermediates break down into compounds with higher oxygen to
326 carbon ratios, such as O3 and O4 attached to only one aromatic ring (Figure 3). For example,
327 degradation of naphthalene initiated via the naphthalene 1,2-dioxygenase pathway produces
328 metabolic intermediates with oxygen numbers as follows: O0 → O2 (two isomers) → O4 → O4
329 (one ring opens) → O2 (lower ring number) → O3 → O4 (towards central metabolism) (Figure
330 3).

331 In this experiment, three O3 compounds, salicylic and 3- and 4-methylsalicylic acids, were the
332 most abundant Level-1 metabolic intermediates (Table S4 and Figure S7). These compounds,
333 however, only account for a small fraction of the DOC (<0.1%), suggesting that: (1) a large
334 proportion of the WSF compounds were unknown and (2) these compounds likely represent a pool
335 of WSF organic carbon that has low concentrations but high flux.

336 To further examine oxygen-containing compounds beyond the level-1 identification, we
337 compared the oxygen distributions of compounds with $C_xH_yO_z$ formulas. Comparisons of relative
338 abundance between each oxygen compound class across time points were based on pair-wise one-
339 tailed Student's t-test. Within the oxygen number distributions of P-WSF_{Total} features, the relative
340 abundances of O4 compounds were significantly higher at T = 7 and 14 than at T = 0 (Figure 4a).
341 Changes in relative abundance of P-WSF_{O-I} features show that most of the production occurred in
342 the O3 and O4 classes (Figure 4b). The relative abundance of O3 P-WSF_M also increased
343 significantly at T = 14, compared to T = 7 (Figure 4d). The oxygen number distribution
344 characteristics from a broader range of compounds in P-WSF_{Total} features are similar to known
345 PAH degradation pathways. Therefore, the high relative abundance of O4 compounds in WSF is
346 likely due to multiple reactions from the degradation of polar and non-polar compounds.

347 The observed oxygen number pattern and complementary genomics data suggest that the
348 degradation of naphthalene and other PAHs in the experiment was likely attributed to dioxygenase-
349 catalyzed reactions. We observed enrichments of multiple genes encoding for dioxygenases in the
350 WSF samples (Figure 5). Although evidence of monooxygenase-catalyzed PAH metabolism is
351 present in some bacteria,^{35, 63} such reactions are predominantly observed in eukaryotic cells such
352 as fungi, yeast, and mammalian cells.⁶⁴⁻⁶⁷ Unlike dioxygenase-encoding genes, we did not observe
353 genes that encode for monooxygenases. The increase in O3 class relative abundance was,
354 therefore, not related to monooxygenases, and is instead more likely to be breakdown products
355 from O4 compounds after the first ring opens. We found that both P-WSF_{O-I} and P-WSF_M features
356 include many O3 compounds (Figure 4b and d). The high abundance of O3 compounds may reflect
357 the production and accumulation of intermediates similar to salicylic acids (i.e. salicylic acid, its
358 methylated forms, and other modifications), which are key metabolites from naphthalene and

359 methyl-naphthalene degradation. Interestingly, the abundance of a subset of O3 compounds also
360 decreased substantially over the course of the experiment within P-WSF_{0-D} (Figure 4c), suggesting
361 some of these compounds were rapidly degraded. These findings suggest that the O3 compound
362 class is a dynamic group of compounds with production, accumulation, and degradation occurring
363 simultaneously.

364 **O3 Metabolites Such as Salicylic Acids Represent a Key Transition Point for WSF**
365 **Degradation.** Salicylic acid is a metabolic intermediate in multiple PAH degradation pathways
366 such as naphthalene, anthracene, fluorene, and phenanthrene; thus, it is reasonable to assume that
367 the degradation of naphthalene, anthracene, fluorene, and phenanthrene in WSF all contributed to
368 the observed concentration of salicylic acid in this study. The methylated forms of salicylic acid
369 (3- and 4-methylsalicylic acids) are key metabolic intermediates in the degradation of 1- and 2-
370 methylnaphthalenes, respectively.

371 The salicylaldehyde dehydrogenase gene (*nahF*, (KEGG, K00152)), which encodes the enzyme
372 that catalyzes the formation of salicylic acid in the naphthalene degradation pathway,^{68, 69} was
373 enriched in the WSF treatments (Figure 5). Further degradation of salicylic acid can proceed via
374 numerous mechanisms, depending on microbial community composition and their associated
375 genes.⁷⁰ For example, in the naphthalene degradation pathway, salicylic acid is transformed into
376 one of two different products through competing reaction mechanisms, i.e. gentistic acid and
377 catechol. We detected trace amounts of gentistic acid in WSF samples (Figure S7), but not
378 catechol. Furthermore, the gene encoding the enzyme for converting salicylic acid to catechol,
379 namely salicylate hydroxylase (*nahG*, (KEGG, K00480)), was not enriched in the WSF samples.

380 Interestingly, the *nahG* gene was elevated in non-WSF samples relative to the WSF treatments
381 (Figure 5), particularly in the VSW treatment. The enrichment of *nahG* gene in the VSW treatment

382 suggest some of the bacteria in seawater retain the genetic capacity to metabolize salicylic acid
383 through the catechol pathway, even though the concentration of salicylic acid in seawater was low.
384 This finding suggests that while the production of salicylic acid via PAH degradation pathways
385 may require specific hydrocarbon-degrading microbial groups, i.e. those that thrive in the presence
386 of WSF, removal of salicylic acid may be mediated by generalist non-oil degrading bacteria. This
387 finding underscores the importance of community structure and succession in complete oil
388 degradation. Distinct groups of oil-degrading microbes are known to bloom at different stages of
389 an oil spill.¹⁵ These microbes potentially produced an array of metabolites that could be utilized
390 by the general microbial community as carbon sources. We propose that while specialized
391 microbes initiate the degradation of WSF, the activity of generalists may be important for the full
392 remineralization of WSF compounds to CO₂. Interestingly, salicylic acid has been shown to
393 enhance the degradation of high molecular weight PAHs,^{38, 71-74} raising the intriguing possibility
394 that salicylic acid stimulates and facilitates degradation of PAHs.

395

396 CONCLUSIONS

397 WSF represents an important component of spilled oil that can play a role in ecotoxicology, and
398 can impact ecosystems,^{3, 5, 75} e.g. in deep-sea oil spills or seepages, in the water column beneath a
399 surface oil slick (Figure 6). The molecular-level understanding of the fate of the polar compounds
400 in crude oil WSF, however, is still scarce. This study offers the first multi-omics insights into
401 microbial degradation of WSF, achieved by integrating a broad suite of chemical features with
402 hydrocarbon-degrading genes.

403 Although this is a controlled laboratory experiment, our results set important reference frames
404 for future oil spill studies and provide new compound targets for field monitoring. The wide range

405 of oxygen-containing WSF compounds share similar oxygen number distributions as those from
406 the degradation of PAHs through dioxygenase pathways. Intermediate metabolites with three
407 oxygen atoms may represent an important transition point in oil degradation in nature. We
408 hypothesize that O3 metabolites such as salicylic acids are funneling compounds for microbial
409 degradation of hydrocarbons. Initial degradation steps may require specialized microbes, but the
410 subsequent metabolism of intermediate products could be achieved by a more diverse group of
411 microbes present in seawater microbial consortia. Consistent with our laboratory findings, we
412 detected salicylic acids and gentistic acid in archived field samples collected in the DWH plume
413 (Table S7), suggesting these compounds may be used as markers for PAH degradation in the field.
414 Additional work with fresh samples or surface oil slicks is needed to confirm these results.
415 Nevertheless, our results highlight the complexity of uncharacterized polar compounds in WSF
416 and their transformation products. The ecotoxicity of this complex pool remains poorly
417 constrained, underscoring the need for improved understanding of the fate and ecotoxicity of WSF
418 on long and short timescales. With more comprehensive knowledge of WSF and its degradation
419 products, markers for assessing the fate and ecotoxicity of spilled oil in the environment can be
420 developed.

421

422 AUTHOR INFORMATION

423 Corresponding Author

424 * Yina Liu

425 Present Addresses

426 # Present address: Geochemical and Environmental Research Group (GERG), Texas A&M
427 University, College Station, TX 77845.

428 Author Contributions

429 The manuscript was written through contributions of all authors. All authors have given approval
430 to the final version of the manuscript. The authors declare no competing financial interest.

431 Supporting Information. Additional experimental details, figures and tables as noted in the text.
432 This material is available free of charge via the Internet at <http://pubs.acs.org>.

433 Funding Sources. This study is funded by the Gulf of Mexico Research Initiative (GOMRI) Project
434 # 161684 to EBK and HKW.

435

436 ACKNOWLEDGMENTS

437 We would like to thank M. Kido Soule for her assistance in the FT-ICR-MS facility, K.
438 Longnecker for her assistance in data processing. G. Swarr and W. Johnson for their help with the
439 extraction efficiency experiment. Data presented in this manuscript is freely available online:
440 doi:10.7266/N71C1TTK (nutrients and DOC data), doi:10.7266/N7N29TW0 (targeted
441 metabolomics data), doi:10.7266/N7WM1BBP (non-targeted metabolomics data), and
442 doi:10.7266/N7W95762 (metagenomic data).

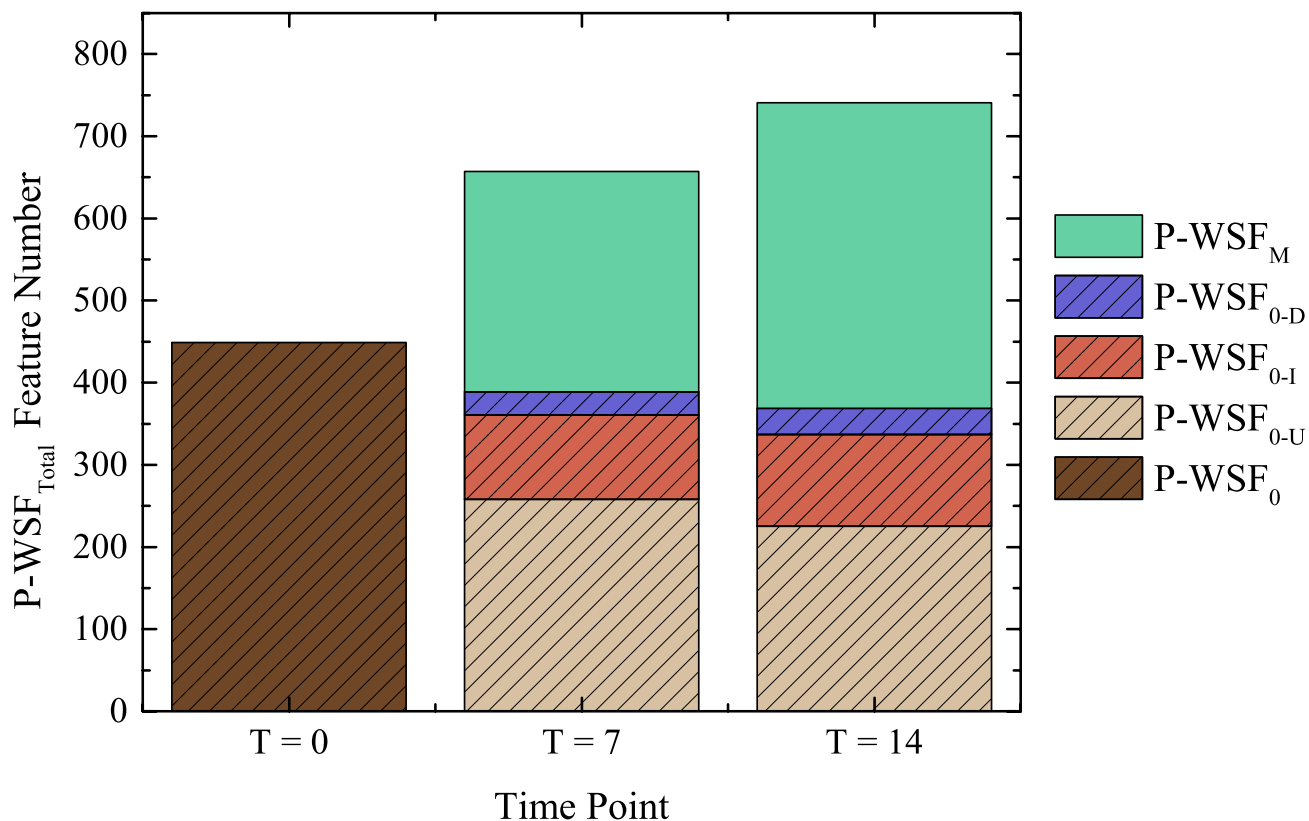
443 ABBREVIATIONS.

444 FT-ICR-MS, Fourier transform ion cyclotron resonance mass spectrometry; VSW, Vineyard
445 Sound seawater; WSF, water-soluble fraction; OTU, operational taxonomic unit; DOC, dissolved
446 organic carbon. WAF, water-accommodated fraction, DOM, dissolved organic matter.

447

448

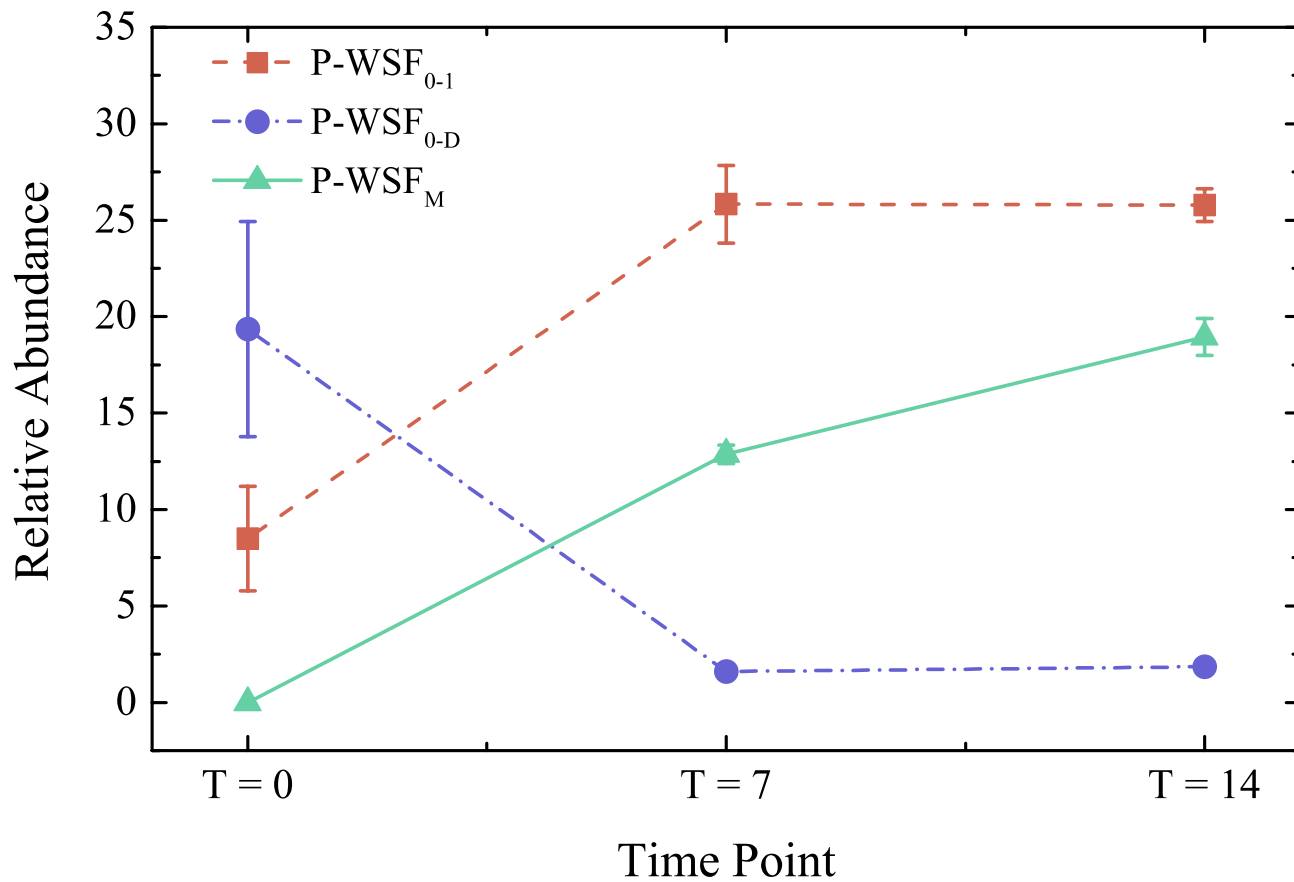
449



450

451 **Figure 1.** Number of observed features across time points T = 0, T = 7, and T = 14 for P-WSF_{Total}.
452 All features shown here were present in all treatment replicates of a time point. Compounds derived
453 from WSF of crude oil at T = 0 (P-WSF₀) are indicated with stripes. Dark brown striped bar
454 represents P-WSF₀ features in the starting material of the incubation experiment. Light brown
455 striped bars highlighted features that persisted from T = 0 to T = 14 and whose relative abundance
456 did not change (P-WSF_{0-U}). Red striped bars highlighted features whose relative abundance
457 increased over the course of the experiment (P-WSF_{0-I}). Blue striped bars highlighted features
458 whose relative abundance decreased the course of the experiment (P-WSF_{0-D}). Green bars
459 highlighted new compounds present at T = 7 and T = 14, but not at T = 0 (P-WSF_M). The difference
460 between the initial striped bar and the sum of the three striped bars at T=7 and T=14 constitutes
461 the features that were lost (P-WSF_{0-C}).

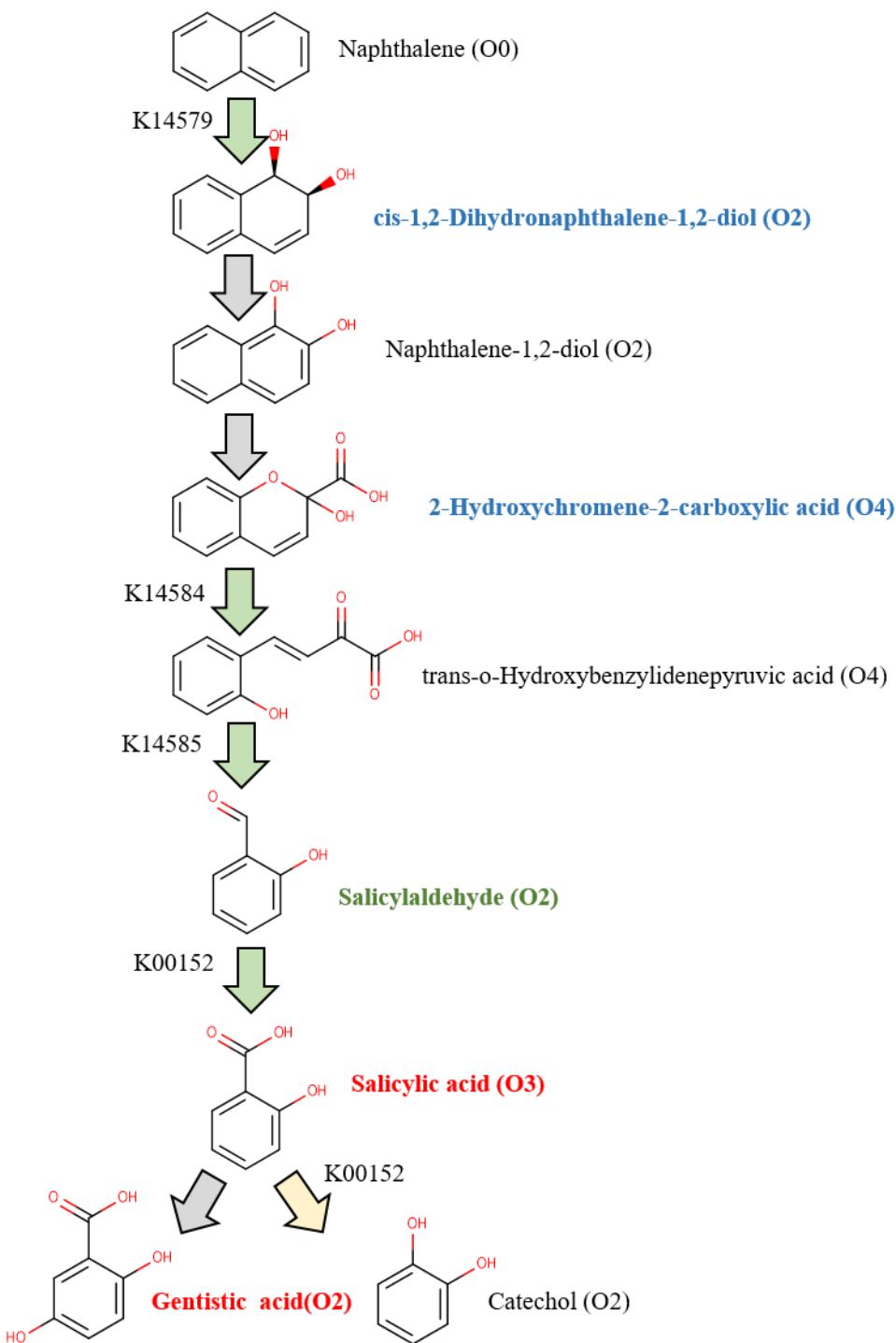
462



463

464 **Figure 2.** Relative abundance of three compound groups observed in WSF treatment (P-WSF₀):
465 P-WSF₀₋₁ (red squares), P-WSF_{0-D} (blue circles), P-WSF_M (green triangles). Error bars represent
466 one standard deviation (n = 3) of relative intensity in each compound class at each time point.

467



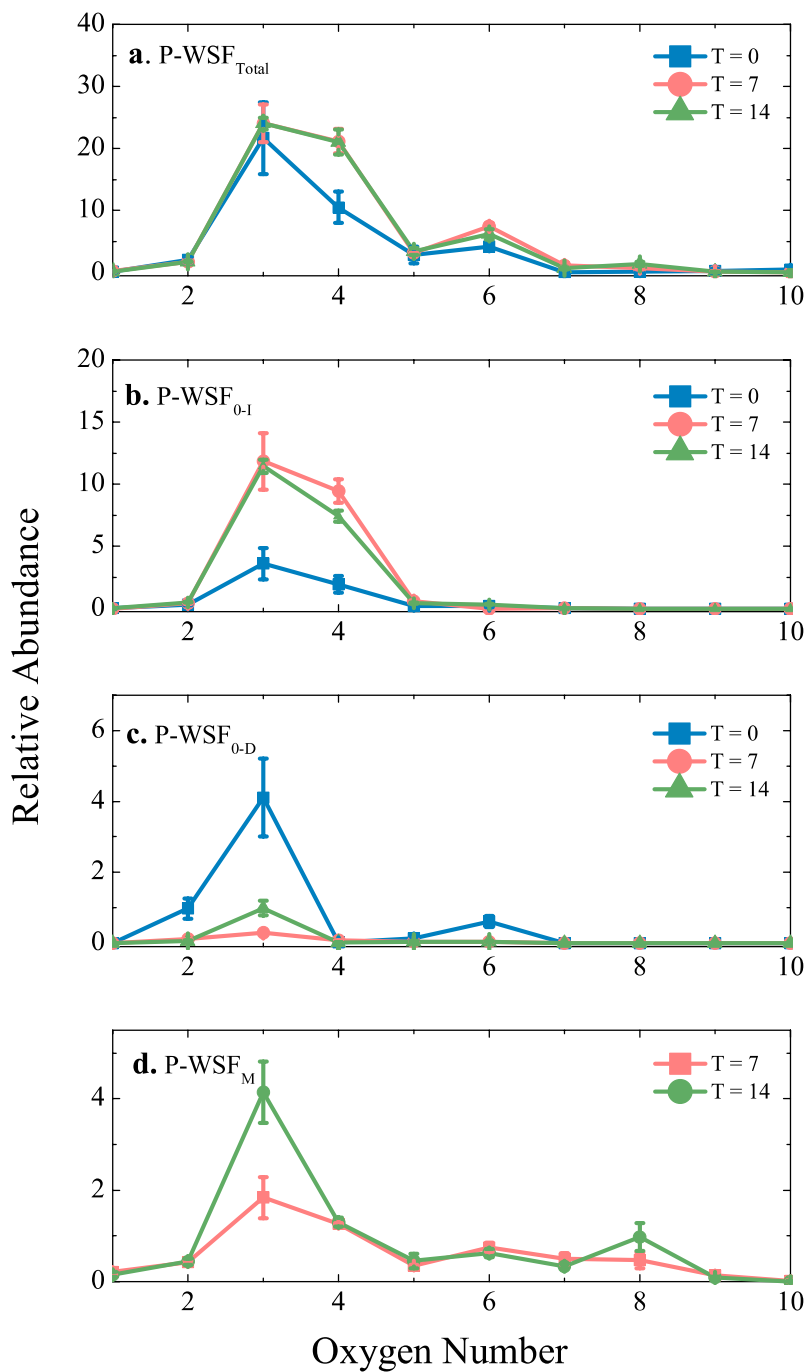
468

469 **Figure 3.** Metabolic pathway of naphthalene degradation initiated through a dioxygenase, based
470 on KEGG. Green arrows indicate the presence of the coding gene encoded in our samples. Grey
471 arrows indicate absence of the coding gene in this study. A yellow arrow indicates the coding gene
472 was observed but not enriched in WSF treatment samples. Chemical names for each structure was
473 labeled with oxygen number indicated in parenthesis. Chemical names in red indicate a level-1
474 identification. Chemical names in green indicate a level-2 putative annotation. Chemical in

475 blue indicate a level-3 putative characterization. Chemical names in black indicated that we did
476 not observe these compounds. BLAST identities of dioxygenase genes detected against an
477 experimentally validated database⁷⁶ are listed in Table S12.

478

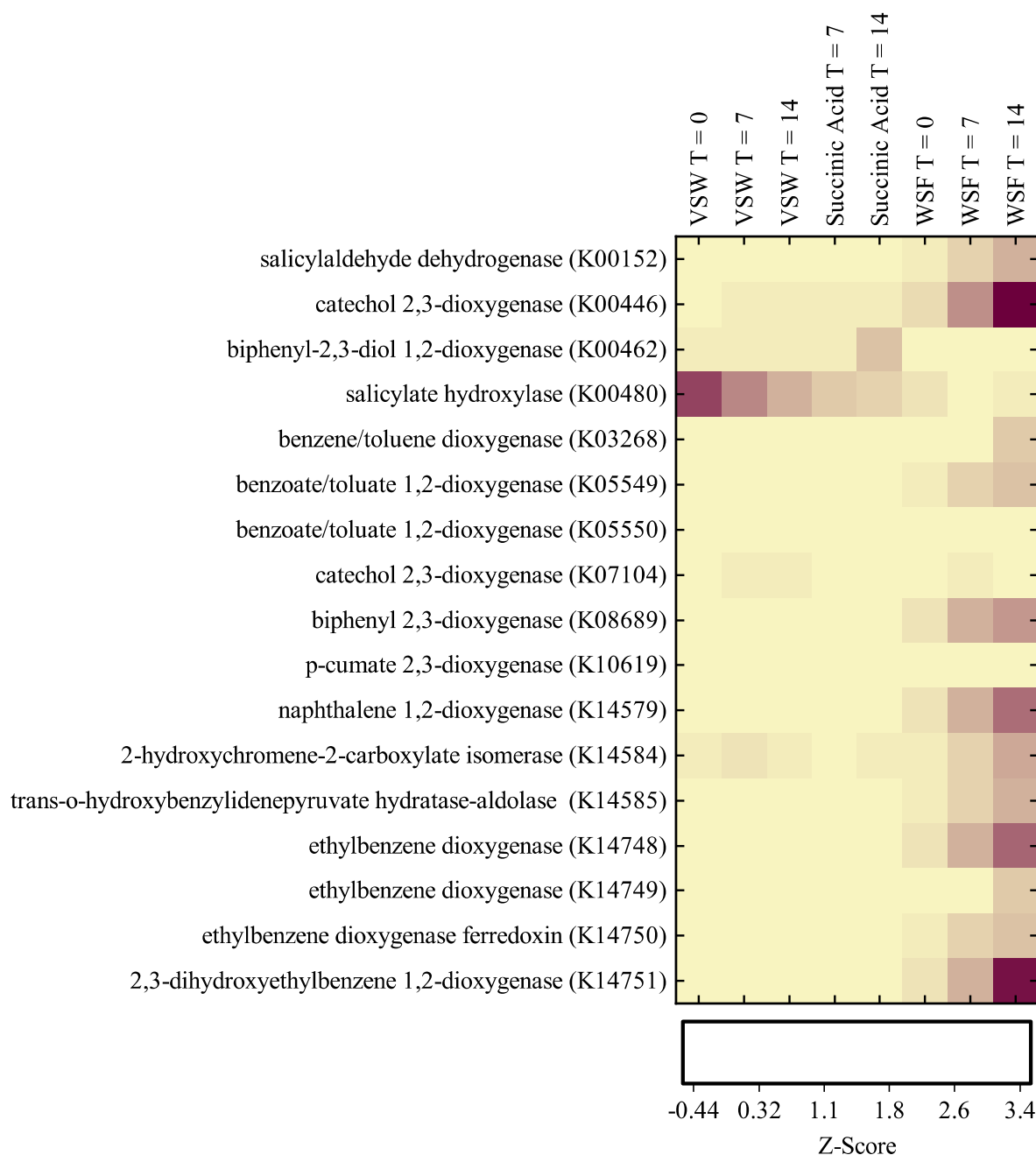
479



480

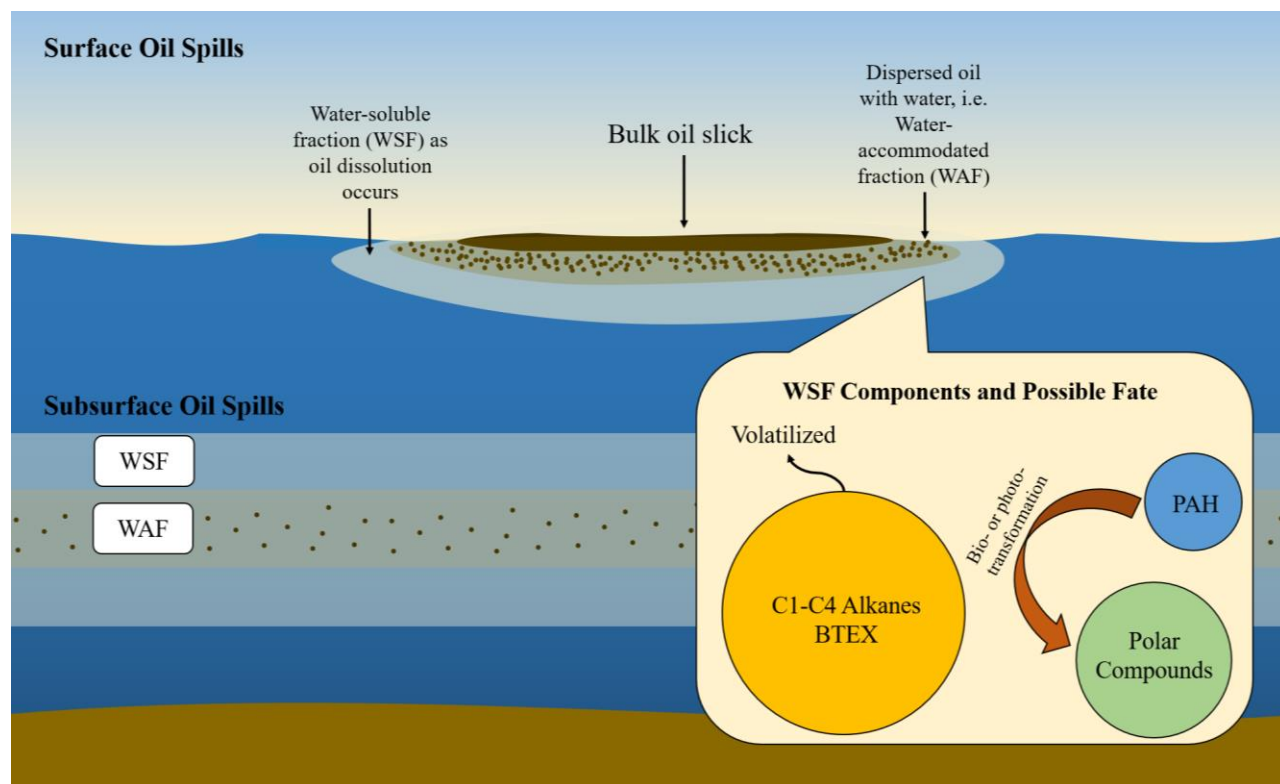
481

482 **Figure 4.** Oxygen number distributions of C_xH_yO_z compounds observed in WSF. (a) P-WSF_{Total},
483 (b) P-WSF₀₋₁, (c) P-WSF_{0-D}, and (d) P-WSF_M in the three time-points (T = 0 in blue, T = 7 in red,
484 and T = 14 in green). Error bars indicate one standard deviation around the mean of triplicate
485 analyses.



486

487 **Figure 5.** Heatmap of genes that encode for aromatic compound metabolisms identified from un-
 488 replicated metagenomic data (described in Supporting Information). Only genes encoding for the
 489 degradation of oil-derived compounds are included. The darker color indicates higher Z-Score
 490 values for specific genes compared to the light yellow. Abundance and percentile of the gene are
 491 listed in Table S11. BLAST identities of dioxygenase genes detected against an experimentally
 492 validated database⁷⁶ are listed in Table S12.



493
494
495 **Figure 6.** Proposed occurrence and fate of the water-soluble fraction (WSF) in the environment.
496 Through dissolution, WSF is expected in the water around the surface oil slicks during an aquatic
497 oil spill. The chemical fingerprint of WSF is distinct from the water-accommodated fraction
498 (WAF), which contained emulsified oil droplets. In the water column, WSF is expected to contain
499 a larger fraction of BTEX, low molecular weight PAHs, and polar compounds. Based on our
500 results, non-polar compounds such as BTEX and PAHs can contribute to polar compounds in WSF
501 through bio-transformation in the water column. At the surface, BTEX may readily volatilize while
502 PAHs are transformed to polar compounds through photo- and bio-mediated pathways.

503 REFERENCE

- 504
- 505 1. National Research Council, *Oil in the Sea III:Inputs, Fates, and Effects*. The National
506 Academies Press: Washington, DC, 2003.
- 507 2. Liu, Y.; Kujawinski, E. B., Chemical Composition and Potential Environmental Impacts
508 of Water-Soluble Polar Crude Oil Components Inferred from ESI FT-ICR MS. *PLoS ONE*
509 **2015**, *10* (9), e0136376.
- 510 3. Melbye, A. G.; Brakstad, O. G.; Hokstad, J. N.; Gregersen, I. K.; Hansen, B. H.; Booth,
511 A. M.; Rowland, S. J.; Tollefsen, K. E., Chemical and Toxicological Characterization of
512 an Unresolved Complex Mixture-Rich Biodegraded Crude Oil. *Environmental Toxicology*
513 *and Chemistry* **2009**, *28* (9), 1815-1824.
- 514 4. Barron, M. G.; Carls, M. G.; Short, J. W.; Rice, S. D., Photoenhanced Toxicity of Aqueous
515 Phase and Chemically Dispersed Weathered Alaska North Slope Crude Oil to Pacific
516 Herring Eggs and Larvae. *Environmental Toxicology and Chemistry* **2003**, *22* (3), 650-660.
- 517 5. Shelton, M. E.; Chapman, P. J.; Foss, S. S.; Fisher, W. S., Degradation of Weathered Oil
518 by Mixed Marine Bacteria and the Toxicity of Accumulated Water-Soluble Material to
519 Two Marine Crustacea. *Archives of Environmental Contamination and Toxicology* **1999**,
520 *36* (1), 13-20.
- 521 6. Maki, H.; Sasaki, T.; Harayama, S., Photo-Oxidation of Biodegraded Crude Oil and
522 Toxicity of the Photo-Oxidized Products. *Chemosphere* **2001**, *44* (5), 1145-1151.
- 523 7. Prince, R. C.; Atlas, R. M., Bioremediation of Marine Oil Spills. *Consequences of*
524 *Microbial Interactions with Hydrocarbons, Oils, and Lipids: Biodegradation and*
525 *Bioremediation* **2018**, 1-25.
- 526 8. Camilli, R.; Reddy, C. M.; Yoerger, D. R.; Van Mooy, B. A. S.; Jakuba, M. V.; Kinsey,
527 J. C.; McIntyre, C. P.; Sylva, S. P.; Maloney, J. V., Tracking Hydrocarbon Plume
528 Transport and Biodegradation at Deepwater Horizon. *Science* **2010**, *330* (6001), 201-204.
- 529 9. Reddy, C. M.; Arey, J. S.; Seewald, J. S.; Sylva, S. P.; Lemkau, K. L.; Nelson, R. K.;
530 Carmichael, C. A.; McIntyre, C. P.; Fenwick, J.; Ventura, G. T.; Van Mooy, B. A. S.;
531 Camilli, R., Composition and Fate of Gas and Oil Released to the Water Column During
532 the *Deepwater Horizon* Oil Spill. *Proceedings of the National Academy of Sciences* **2012**,
533 *109* (50), 20229-20234.
- 534 10. Ryerson, T. B.; Camilli, R.; Kessler, J. D.; Kujawinski, E. B.; Reddy, C. M.; Valentine,
535 D. L.; Atlas, E.; Blake, D. R.; de Gouw, J.; Meinardi, S.; Parrish, D. D.; Peischl, J.;
536 Seewald, J. S.; Warneke, C., Chemical Data Quantify *Deepwater Horizon* Hydrocarbon
537 Flow Rate and Environmental Distribution. *Proceedings of the National Academy of*
538 *Sciences* **2012**.

- 539 11. Valentine, D. L.; Kessler, J. D.; Redmond, M. C.; Mendes, S. D.; Heintz, M. B.; Farwell,
540 C.; Hu, L.; Kinnaman, F. S.; Yvon-Lewis, S.; Du, M.; Chan, E. W.; Tigreros, F. G.;
541 Villanueva, C. J., Propane Respiration Jump-Starts Microbial Response to a Deep Oil Spill.
542 *Science* **2010**, *330* (6001), 208-211.
- 543 12. Aeppli, C.; Carmichael, C. A.; Nelson, R. K.; Lemkau, K. L.; Graham, W. M.; Redmond,
544 M. C.; Valentine, D. L.; Reddy, C. M., Oil Weathering after the *Deepwater Horizon*
545 Disaster Led to the Formation of Oxygenated Residues. *Environ Sci Technol* **2012**, *46* (16),
546 8799-8807.
- 547 13. Spier, C.; Stringfellow, W. T.; Hazen, T. C.; Conrad, M., Distribution of Hydrocarbons
548 Released During the 2010 MC252 Oil Spill in Deep Offshore Waters. *Environmental*
549 *Pollution* **2013**, *173*, 224-230.
- 550 14. Kleindienst, S.; Seidel, M.; Ziervogel, K.; Grim, S.; Loftis, K.; Harrison, S.; Malkin, S.
551 Y.; Perkins, M. J.; Field, J.; Sogin, M. L.; Dittmar, T.; Passow, U.; Medeiros, P. M.;
552 Joye, S. B., Chemical Dispersants Can Suppress the Activity of Natural Oil-Degrading
553 Microorganisms. *Proceedings of the National Academy of Sciences* **2015**, *112* (48), 14900-
554 14905.
- 555 15. Dubinsky, E. A.; Conrad, M. E.; Chakraborty, R.; Bill, M.; Borglin, S. E.; Hollibaugh,
556 J. T.; Mason, O. U.; Piceno, Y.; Reid, F. C.; Stringfellow, W. T.; Tom, L. M.; Hazen,
557 T. C.; Andersen, G. L., Succession of Hydrocarbon-Degrading Bacteria in the Aftermath
558 of the *Deepwater Horizon* Oil Spill in the Gulf of Mexico. *Environ Sci Technol* **2013**, *47*
559 (19), 10860-10867.
- 560 16. Hazen, T. C.; Dubinsky, E. A.; DeSantis, T. Z.; Andersen, G. L.; Piceno, Y. M.; Singh,
561 N.; Jansson, J. K.; Probst, A.; Borglin, S. E.; Fortney, J. L.; Stringfellow, W. T.; Bill,
562 M.; Conrad, M. E.; Tom, L. M.; Chavarria, K. L.; Alusi, T. R.; Lamendella, R.; Joyner,
563 D. C.; Spier, C.; Baelum, J.; Auer, M.; Zemla, M. L.; Chakraborty, R.; Sonnenthal, E.
564 L.; D'haeseleer, P.; Holman, H.-Y. N.; Osman, S.; Lu, Z.; Van Nostrand, J. D.; Deng,
565 Y.; Zhou, J.; Mason, O. U., Deep-Sea Oil Plume Enriches Indigenous Oil-Degrading
566 Bacteria. *Science* **2010**, *330* (6001), 204-208.
- 567 17. Mason, O. U.; Hazen, T. C.; Borglin, S.; Chain, P. S. G.; Dubinsky, E. A.; Fortney, J.
568 L.; Han, J.; Holman, H.-Y. N.; Hultman, J.; Lamendella, R.; Mackelprang, R.; Malfatti,
569 S.; Tom, L. M.; Tringe, S. G.; Woyke, T.; Zhou, J.; Rubin, E. M.; Jansson, J. K.,
570 Metagenome, Metatranscriptome and Single-Cell Sequencing Reveal Microbial Response
571 to *Deepwater Horizon* Oil Spill. *ISME J* **2012**, *6* (9), 1715-1727.
- 572 18. Incardona, J. P.; Vines, C. A.; Anulacion, B. F.; Baldwin, D. H.; Day, H. L.; French, B.
573 L.; Labenia, J. S.; Linbo, T. L.; Myers, M. S.; Olson, O. P.; Sloan, C. A.; Sol, S.;
574 Griffin, F. J.; Menard, K.; Morgan, S. G.; West, J. E.; Collier, T. K.; Ylitalo, G. M.;
575 Cherr, G. N.; Scholz, N. L., Unexpectedly High Mortality in Pacific Herring Embryos
576 Exposed to the 2007 Cosco Busan Oil Spill in San Francisco Bay. *Proceedings of the*
577 *National Academy of Sciences* **2012**, *109* (2), E51-E58.

- 578 19. Reisfeld, A.; Rosenberg, E.; Gutnick, D., Microbial Degradation of Crude Oil: Factors
579 Affecting the Dispersion in Sea Water by Mixed and Pure Cultures. *Applied Microbiology*
580 **1972**, *24* (3), 363.
- 581 20. Atlas, R. M., Petroleum Biodegradation and Oil Spill Bioremediation. *Marine Pollution*
582 *Bulletin* **1995**, *31* (4), 178-182.
- 583 21. Atlas, R. M.; Hazen, T. C., Oil Biodegradation and Bioremediation: A Tale of the Two
584 Worst Spills in U.S. History. *Environ Sci Technol* **2011**, *45* (16), 6709-6715.
- 585 22. Atlas, R. M., Microbial Hydrocarbon Degradation—Bioremediation of Oil Spills. *Journal*
586 *of Chemical Technology & Biotechnology* **1991**, *52* (2), 149-156.
- 587 23. Bagby, S. C.; Reddy, C. M.; Aeppli, C.; Fisher, G. B.; Valentine, D. L., Persistence and
588 Biodegradation of Oil at the Ocean Floor Following **Deepwater Horizon**. *Proceedings of*
589 *the National Academy of Sciences* **2017**, *114* (1), E9.
- 590 24. Redmond, M. C.; Valentine, D. L., Natural Gas and Temperature Structured a Microbial
591 Community Response to the *Deepwater Horizon* Oil Spill. *Proceedings of the National*
592 *Academy of Sciences* **2012**, *109* (50), 20292-20297.
- 593 25. Venosa, A. D.; Campo, P.; Suidan, M. T., Biodegradability of Lingering Crude Oil 19
594 Years after the Exxon Valdez Oil Spill. *Environ Sci Technol* **2010**, *44*.
- 595 26. Kimes, N. E.; Callaghan, A. V.; Aktas, D. F.; Smith, W. L.; Sunner, J.; Golding, B.;
596 Drozdowska, M.; Hazen, T. C.; Suflita, J. M.; Morris, P. J., Metagenomic Analysis and
597 Metabolite Profiling of Deep–Sea Sediments from the Gulf of Mexico Following the
598 *Deepwater Horizon* Oil Spill. *Frontiers in Microbiology* **2013**, *4*, 50.
- 599 27. Kostka, J. E.; Prakash, O.; Overholt, W. A.; Green, S. J.; Freyer, G.; Canion, A.;
600 Delgardio, J.; Norton, N.; Hazen, T. C.; Huettel, M., Hydrocarbon-Degrading Bacteria
601 and the Bacterial Community Response in Gulf of Mexico Beach Sands Impacted by the
602 *Deepwater Horizon* Oil Spill. *Appl. Environ. Microbiol.* **2011**, *77* (22), 7962-7974.
- 603 28. Seidel, M.; Kleindienst, S.; Dittmar, T.; Joye, S. B.; Medeiros, P. M., Biodegradation of
604 Crude Oil and Dispersants in Deep Seawater from the Gulf of Mexico: Insights from Ultra-
605 High Resolution Mass Spectrometry. *Deep Sea Research Part II: Topical Studies in*
606 *Oceanography* **2016**, *129*, 108-118.
- 607 29. Chen, H.; Hou, A.; Corilo, Y. E.; Lin, Q.; Lu, J.; Mendelssohn, I. A.; Zhang, R.;
608 Rodgers, R. P.; McKenna, A. M., 4 Years after the *Deepwater Horizon* Spill: Molecular
609 Transformation of Macondo Well Oil in Louisiana Salt Marsh Sediments Revealed by FT-
610 ICR Mass Spectrometry. *Environ Sci Technol* **2016**.
- 611 30. Aeppli, C.; Nelson, R. K.; Radović, J. R.; Carmichael, C. A.; Valentine, D. L.; Reddy,
612 C. M., Recalcitrance and Degradation of Petroleum Biomarkers Upon Abiotic and Biotic

- 613 Natural Weathering of *Deepwater Horizon* Oil. *Environ Sci Technol* **2014**, *48* (12), 6726-
614 6734.
- 615 31. Hughey, C. A.; Rodgers, R. P.; Marshall, A. G.; Qian, K.; Robbins, W. K., Identification
616 of Acidic NSO Compounds in Crude Oils of Different Geochemical Origins by Negative
617 Ion Electrospray Fourier Transform Ion Cyclotron Resonance Mass Spectrometry. *Organic*
618 *Geochemistry* **2002**, *33* (7), 743-759.
- 619 32. Siron, R.; Rontani, J. F.; Giusti, G., Chemical Characterization of a Water Soluble Fraction
620 (WSF) of Crude Oil. *Toxicological & Environmental Chemistry* **1987**, *15* (3), 223-229.
- 621 33. Stanford, L. A.; Kim, S.; Klein, G. C.; Smith, D. F.; Rodgers, R. P.; Marshall, A. G.,
622 Identification of Water-Soluble Heavy Crude Oil Organic-Acids, Bases, and Neutrals by
623 Electrospray Ionization and Field Desorption Ionization Fourier Transform Ion Cyclotron
624 Resonance Mass Spectrometry. *Environ Sci Technol* **2007**, *41* (8), 2696-2702.
- 625 34. Ray, P. Z.; Chen, H.; Podgorski, D. C.; McKenna, A. M.; Tarr, M. A., Sunlight Creates
626 Oxygenated Species in Water-Soluble Fractions of *Deepwater Horizon* Oil. *J Hazard*
627 *Mater* **2014**, *280* (0), 636-643.
- 628 35. Mason, O.; Han, J.; Woyke, T.; Jansson, J., Single-Cell Genomics Reveals Features of a
629 *Colwellia* Species that was Dominant During the *Deepwater Horizon* Oil Spill. *Frontiers*
630 *in Microbiology* **2014**, *5*.
- 631 36. Wang, L.; Qiao, N.; Sun, F.; Shao, Z., Isolation, Gene Detection and Solvent Tolerance
632 of Benzene, Toluene and Xylene Degrading Bacteria from Nearshore Surface Water and
633 Pacific Ocean Sediment. *Extremophiles* **2008**, *12* (3), 335-342.
- 634 37. Kappell, A. D.; Wei, Y.; Newton, R. J.; Van Nostrand, J. D.; Zhou, J.; McLellan, S. L.;
635 Hristova, K. R., The Polycyclic Aromatic Hydrocarbon Degradation Potential of Gulf of
636 Mexico Native Coastal Microbial Communities after the *Deepwater Horizon* Oil Spill.
637 *Frontiers in Microbiology* **2014**, *5*, 205.
- 638 38. Ghosal, D.; Ghosh, S.; Dutta, T. K.; Ahn, Y., Current State of Knowledge in Microbial
639 Degradation of Polycyclic Aromatic Hydrocarbons (PAHs): A Review. *Frontiers in*
640 *Microbiology* **2016**, *7*, 1369.
- 641 39. Kessler, J. D.; Valentine, D. L.; Redmond, M. C.; Du, M.; Chan, E. W.; Mendes, S. D.;
642 Quiroz, E. W.; Villanueva, C. J.; Shusta, S. S.; Werra, L. M.; Yvon-Lewis, S. A.; Weber,
643 T. C., A Persistent Oxygen Anomaly Reveals the Fate of Spilled Methane in the Deep Gulf
644 of Mexico. *Science* **2011**, *331* (6015), 312-315.
- 645 40. Vaughan, P. P.; Wilson, T.; Kamerman, R.; Hagy, M. E.; McKenna, A.; Chen, H.;
646 Jeffrey, W. H., Photochemical Changes in Water Accommodated Fractions of MC252 and
647 Surrogate Oil Created During Solar Exposure as Determined by FT-ICR MS. *Marine*
648 *Pollution Bulletin* **2016**.

- 649 41. Hughey, C. A.; Rodgers, R. P.; Marshall, A. G.; Walters, C. C.; Qian, K.; Mankiewicz,
650 P., Acidic and Neutral Polar Nso Compounds in Smackover Oils of Different Thermal
651 Maturity Revealed by Electrospray High Field Fourier Transform Ion Cyclotron
652 Resonance Mass Spectrometry. *Org. Geochem.* **2004**, *35* (7), 863-880.
- 653 42. McKenna, A. M.; Nelson, R. K.; Reddy, C. M.; Savory, J. J.; Kaiser, N. K.; Fitzsimmons,
654 J. E.; Marshall, A. G.; Rodgers, R. P., Expansion of the Analytical Window for Oil Spill
655 Characterization by Ultrahigh Resolution Mass Spectrometry: Beyond Gas
656 Chromatography. *Environ. Sci. Technol.* **2013**, *47* (13), 7530-7539.
- 657 43. Rodgers, R.; Marshall, A., Petroleomics: Advanced Characterization of Petroleum-Derived
658 Materials by Fourier Transform Ion Cyclotron Resonance Mass Spectrometry (FT-ICR
659 MS). In *Asphaltenes, Heavy Oils, and Petroleomics*, Mullins, O.; Sheu, E.; Hammami,
660 A.; Marshall, A., Eds. Springer New York: 2007; pp 63-93.
- 661 44. Marshall, A. G.; Rodgers, R. P., Petroleomics: Chemistry of the Underworld. *Proc. Natl.*
662 *Acad. Sci.* **2008**, *105* (47), 18090-18095.
- 663 45. Du, M.; Kessler, J. D., Assessment of the Spatial and Temporal Variability of Bulk
664 Hydrocarbon Respiration Following the *Deepwater Horizon* Oil Spill. *Environmental*
665 *Science & Technology* **2012**, *46* (19), 10499-10507.
- 666 46. Zhou, Z.; Guo, L.; Shiller, A. M.; Lohrenz, S. E.; Asper, V. L.; Osburn, C. L.,
667 Characterization of Oil Components from the *Deepwater Horizon* Oil Spill in the Gulf of
668 Mexico Using Fluorescence Eem and Parafac Techniques. *Mar Chem* **2013**, *148*, 10-21.
- 669 47. Nelson, C. E.; Carlson, C. A., Tracking Differential Incorporation of Dissolved Organic
670 Carbon Types among Diverse Lineages of Sargasso Sea Bacterioplankton. *Environmental*
671 *Microbiology* **2012**, *14* (6), 1500-1516.
- 672 48. Vaughan, P. P.; Wilson, T.; Kamerman, R.; Hagy, M. E.; McKenna, A.; Chen, H.;
673 Jeffrey, W. H., Photochemical Changes in Water Accommodated Fractions of MC252 and
674 Surrogate Oil Created During Solar Exposure as Determined by FT-ICR MS. *Marine*
675 *Pollution Bulletin* **2016**, *104* (1), 262-268.
- 676 49. Dittmar, T.; Koch, B.; Hertkorn, N.; Kattner, G., A Simple and Efficient Method for the
677 Solid-Phase Extraction of Dissolved Organic Matter (SPE-DOM) from Seawater. *Limnol.*
678 *Oceanogr. Methods* **2008**, *6*, 230-235.
- 679 50. Longnecker, K., Dissolved Organic Matter in Newly Formed Sea Ice and Surface
680 Seawater. *Geochim Cosmochim Acta* **2015**, *171*, 39-49.
- 681 51. Johnson, W. M.; Kido Soule, M. C.; Kujawinski, E. B., Extraction Efficiency and
682 Quantification of Dissolved Metabolites in Targeted Marine Metabolomics. *Limnology and*
683 *Oceanography: Methods* **2017**, n/a-n/a.

- 684 52. Kido Soule, M. C.; Longnecker, K.; Johnson, W. M.; Kujawinski, E. B., Environmental
685 Metabolomics: Analytical Strategies. *Mar Chem* **2015**, *177*, Part 2, 374-387.
- 686 53. Sumner, L. W.; Amberg, A.; Barrett, D.; Beale, M. H.; Beger, R.; Daykin, C. A.; Fan,
687 T. W. M.; Fiehn, O.; Goodacre, R.; Griffin, J. L.; Hankemeier, T.; Hardy, N.; Harnly,
688 J.; Higashi, R.; Kopka, J.; Lane, A. N.; Lindon, J. C.; Marriott, P.; Nicholls, A. W.;
689 Reily, M. D.; Thaden, J. J.; Viant, M. R., Proposed Minimum Reporting Standards for
690 Chemical Analysis. *Metabolomics* **2007**, *3* (3), 211-221.
- 691 54. Ruttkies, C.; Schymanski, E. L.; Wolf, S.; Hollender, J.; Neumann, S., Metfrag
692 Relunched: Incorporating Strategies Beyond *in Silico* Fragmentation. *Journal of*
693 *Cheminformatics* **2016**, *8* (1), 3.
- 694 55. Kujawinski, E. B.; Behn, M. D., Automated Analysis of Electrospray Ionization Fourier
695 Transform Ion Cyclotron Resonance Mass Spectra of Natural Organic Matter. *Analytical*
696 *Chemistry* **2006**, *78* (13), 4363-4373.
- 697 56. Pelz, O.; Brown, J.; Huddleston, M.; Rand, G.; Gardinali, P.; Stubblefield, W.;
698 BenKinney, M. T.; Ahnell, A.; Bp Gcro, H.; Exponent, M., Selection of a Surrogate
699 MC252 Oil as a Reference Material for Future Aquatic Toxicity Tests and Other Studies.
700 *survival* **2011**, *20*, 25-000.
- 701 57. Hazen, T. C.; Dubinsky, E. A.; Desantis, T. Z.; Andersen, G. L.; Piceno, Y. M.; Singh,
702 N.; Jansson, J. K.; Probst, A.; Borglin, S. E.; Fortney, J. L.; Stringfellow, W. T.; Bill,
703 M.; Conrad, M. E.; Tom, L. M.; Chavarria, K. L.; Alusi, T. R.; Lamendella, R.; Joyner,
704 D. C.; Spier, C.; Baelum, J.; Auer, M.; Zemla, M. L.; Chakraborty, R.; Sonnenthal, E.
705 L.; D'Haeseleer, P.; Holman, H. Y.; Osman, S.; Lu, Z.; Van Nostrand, J. D.; Deng, Y.;
706 Zhou, J.; Mason, O. U., Deep-Sea Oil Plume Enriches Indigenous Oil- Degrading Bacteria.
707 *Science* **2010**, *330*.
- 708 58. Kelley, I.; Freeman, J.; Cerniglia, C., Identification of Metabolites from Degradation of
709 Naphthalene by a *Mycobacterium Sp.* *Biodegradation* **1990**, *1* (4), 283-290.
- 710 59. Cerniglia, C. E., Biodegradation of Polycyclic Aromatic Hydrocarbons. *Current Opinion*
711 *in Biotechnology* **1993**, *4* (3), 331-338.
- 712 60. Eaton, R. W., Organization and Evolution of Naphthalene Catabolic Pathways: Sequence
713 of the DNA Encoding 2-Hydroxychromene-2-Carboxylate Isomerase and Trans-O-
714 Hydroxybenzylidenepyruvate Hydratase-Aldolase from the *Nah7* Plasmid. *Journal of*
715 *bacteriology* **1994**, *176* (24), 7757-7762.
- 716 61. Kimes, N. E.; Callaghan, A. V.; Suflita, J. M.; Morris, P. J., Microbial Transformation of
717 the *Deepwater Horizon* Oil Spill – Past, Present, and Future Perspectives. *Frontiers in*
718 *Microbiology* **2014**, *5*.

- 719 62. Eaton, R. W.; Chapman, P. J., Bacterial Metabolism of Naphthalene: Construction and Use
720 of Recombinant Bacteria to Study Ring Cleavage of 1,2-Dihydroxynaphthalene and
721 Subsequent Reactions. *Journal of Bacteriology* **1992**, *174* (23), 7542-7554.
- 722 63. Ressler, B. P.; Kneifel, H.; Winter, J., Bioavailability of Polycyclic Aromatic
723 Hydrocarbons and Formation of Humic Acid-Like Residues During Bacterial PAH
724 Degradation. *Appl Microbiol Biotechnol* **1999**, *53* (1), 85-91.
- 725 64. Cerniglia, C.; Crow, S., Metabolism of Aromatic Hydrocarbons by Yeasts. *Archives of*
726 *Microbiology* **1981**, *129* (1), 9-13.
- 727 65. Cerniglia, C.; Freeman, J. P.; Evans, F., Evidence for an Arene Oxide-Nih Shift Pathway
728 in the Transformation of Naphthalene to 1-Naphthol by *Bacillus Cereus*. *Archives of*
729 *Microbiology* **1984**, *138* (4), 283-286.
- 730 66. Jerina, D. M.; Daly, J. W., Arene Oxides: A New Aspect of Drug Metabolism. *Science*
731 **1974**, *185* (4151), 573-582.
- 732 67. Syed, K.; Doddapaneni, H.; Subramanian, V.; Lam, Y. W.; Yadav, J. S., Genome-to-
733 Function Characterization of Novel Fungal P450 Monooxygenases Oxidizing Polycyclic
734 Aromatic Hydrocarbons (PAHs). *Biochemical and Biophysical Research Communications*
735 **2010**, *399* (4), 492-497.
- 736 68. Kiyohara, H.; Nagao, K., The Catabolism of Phenanthrene and Naphthalene by Bacteria.
737 *Microbiology* **1978**, *105* (1), 69-75.
- 738 69. Evans, W. C.; Fernley, H. N.; Griffiths, E., Oxidative Metabolism of Phenanthrene and
739 Anthracene by Soil Pseudomonads. The Ring-Fission Mechanism. *Biochemical Journal*
740 **1965**, *95* (3), 819-831.
- 741 70. Monticello, D. J.; Bakker, D.; Schell, M.; Finnerty, W. R., Plasmid-Borne Tn5 Insertion
742 Mutation Resulting in Accumulation of Gentisate from Salicylate. *Appl. Environ.*
743 *Microbiol.* **1985**, *49* (4), 761-764.
- 744 71. Weissenfels, W. D.; Beyer, M.; Klein, J.; Rehm, H. J., Microbial Metabolism of
745 Fluoranthene: Isolation and Identification of Ring Fission Products. *Applied Microbiology*
746 *and Biotechnology* **1991**, *34* (4), 528-535.
- 747 72. Juhasz, A. L.; Naidu, R., Bioremediation of High Molecular Weight Polycyclic Aromatic
748 Hydrocarbons: A Review of the Microbial Degradation of Benzo[a]Pyrene. *International*
749 *Biodeterioration & Biodegradation* **2000**, *45* (1), 57-88.
- 750 73. Chen, S.-H.; Aitken, M. D., Salicylate Stimulates the Degradation of High-Molecular
751 Weight Polycyclic Aromatic Hydrocarbons by *Pseudomonas Saccharophila* P15.
752 *Environmental Science & Technology* **1999**, *33* (3), 435-439.

- 753 74. Rentz, J. A.; Alvarez, P. J. J.; Schnoor, J. L., Benzo[a]Pyrene Degradation by
754 Sphingomonas Yanoikuyae Jar02. *Environmental Pollution* **2008**, *151* (3), 669-677.
- 755 75. Kennedy, C. J.; Farrell, A. P., Ion Homeostasis and Interrenal Stress Responses in Juvenile
756 Pacific Herring, *Clupea Pallasii*, Exposed to the Water-Soluble Fraction of Crude Oil.
757 *Journal of Experimental Marine Biology and Ecology* **2005**, *323* (1), 43-56.
- 758 76. Meynet, P.; Head, I. M.; Werner, D.; Davenport, R. J., Re-Evaluation of Dioxygenase
759 Gene Phylogeny for the Development and Validation of a Quantitative Assay for
760 Environmental Aromatic Hydrocarbon Degradation. *FEMS microbiology ecology* **2015**, *91*
761 (6), fiv049.
- 762